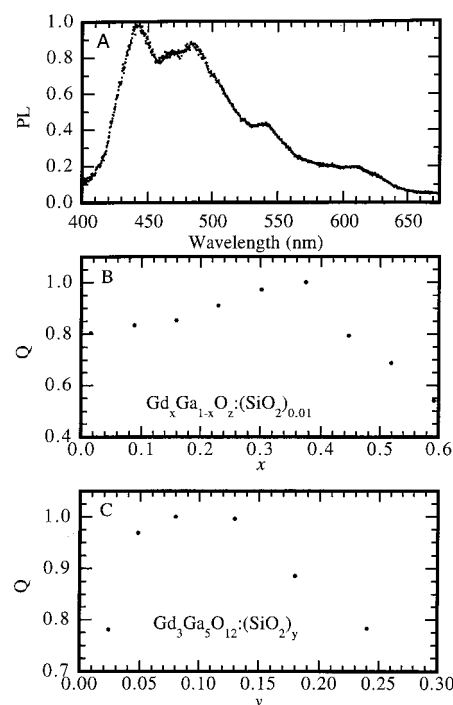samples treated as above or at 1100°C for >32 hours showed no trace of crystalline silicate by XRD and have very weak luminescence (in contrast to the films), and the optimal stoichiometry coincides with $Gd_3Ga_5O_{12}$. However, x-ray photoemission spectroscopy (XPS) and energy-dispersive x-ray analysis confirmed the presence of SiO_2 in the sample. The measured percentage of SiO_2 in the sample was higher than that expected from the deposition stoichiometry, which suggests that SiO_2 is on the surfaces of the particles of $Gd_3Ga_5O_{12}$. XPS measurements also ruled out the presence of residual carbon in the sample. Consistent with these results, pure Gd_2O_3, Ga_2O_3 and $Gd_3Ga_5O_{12}$ thin films made on an $LaAlO_3$ substrate using the same procedures showed no PL in the same spectral region.

It is well known that both oxidized porous silicon (p-Si) (9, 10) and properly prepared silicon oxide (11–13) show blue photoluminescence at 420 to 490 nm.

Two models have been proposed to explain the blue PL from p-Si. The first model (10), used to explain the photoluminescence in SiO_x, connects the blue emission in p-Si directly to the defect states of SiO_2. In the second model [the extended quantum confinement (EQC) model], the PL arises from charge recombination processes across the broadened band gap of nanocrystalline Si (14). In our blue PL samples, the EQC model can be excluded because there is no pure Si in the sample. There are two possible origins for the blue PL in $Gd_3Ga_5O_{12}/SiO_2$. First, it is possible that Si may have substituted into the tetrahedral sites of Ga and functions as the activator in the host lattice of $Gd_3Ga_5O_{12}$. This notion is less likely because we are not aware of any report of Si-activated phosphors. It is more likely that nanocrystalline or amorphous SiO_2 or interfacial silicate (therefore not detectable by XRD) is finely dispersed into the $Gd_3Ga_5O_{12}$ matrix and possibly coated on the surface of $Gd_3Ga_5O_{12}$ grains, which are on the order of 100 nm as observed by atomic force microscopy. These interfaces may form the specific local electron states that give rise to the observed blue emission. Consistent with this notion, etching of the $Gd_3Ga_5O_{12}/SiO_2$ films with dilute hydrofluoric acid (which does not substantially affect the $Gd_3Ga_5O_{12}$ host) dramatically reduces photoluminescence in comparison to that in the untreated films. Additional experimental and theoretical investigations are needed to more fully understand the mechanism of luminescence in this material. Given the high PL efficiency and compatibility of the synthesis methods with Si wafer processing, this material may find applications in optoelectronics and imaging technologies.

REFERENCES AND NOTES

1. G. Blasse and B. C. Grabmaier, *Luminescent Materials* (Springer-Verlag, Berlin, 1994).
2. X.-D. Xiang *et al.*, *Science* **268**, 1738 (1995); G. Briceño, H. Chang, X. Sun, P. G. Schultz, X.-D. Xiang, *ibid.* **270**, 273 (1995).
3. E. Danielson *et al.*, *Nature* **389**, 944 (1997).
4. T. Wei, X.-D. Xiang, W. G. Wallace-Freedman, P. G. Schultz, X.-D. Xiang, *Appl. Phys. Lett.* **68**, 3506 (1996); H. Chang *et al.*, in preparation.
5. F. C. Moates *et al.*, *Ind. Eng. Chem. Res.* **35**, 4801 (1996).
6. X.-D. Sun *et al.*, *Adv. Mater.* **9**, 1046 (1997).
7. L. Fister, T. Novet, C. A. Grant, D. C. Johnson, *Advances in the Synthesis and Reactivity of the Solids* (JAI, New York, 1994), vol. 2, pp. 155–234.
8. R. T. Collins, P. M. Fauchet, M. A. Tischler, *Phys. Today* **50**, 24 (1997).
9. T. Ito, T. Ohta, A. Hiraki, *Jpn. J. Appl. Phys.* **31**, L1 (1992).
10. L. Tsybeskov, Ju. V. Vandyshev, P. M. Fauchet, *Phys. Rev. B* **49**, 7821 (1994).
11. J. H. Stathis and M. A. Kastener, *ibid.* **35**, 2972 (1987).
12. R. Tohmon *et al.*, *Phys. Rev. Lett.* **62**, 1388 (1989); H. Nishikawa, T. Shiroyma, R. Nakamura, Y. Ohki, *Phys. Rev. B* **45**, 586 (1992).
13. G. G. Qin *et al.*, *Phys. Rev. B* **55**, 12876 (1997).
14. F. Koch, in *Materials Research Society Symposia Proceedings No. 298*, M. A. Tischler, R. T. Collins, M. L. Thewalt, G. Abstreiter, Eds. (Materials Research Society, Pittsburgh, PA, 1993), p. 319.
15. We thank W. D. Hinsberg for helpful advice. This work was supported by the Office of Naval Research; by the Director, Office of Energy Research, Office of Basic Energy Research, Division of Materials Sciences, of the U.S. Department of Energy; and by the W. M. Keck foundation.

Fig. 3. (**A**) Photoluminescent spectrum of a sample site (31, 3) from the quaternary library [nominal composition $Gd_{5.2}Ga_{3.33}O_z$ under UV excitation at maximum wavelength (λ_{max}) (258 nm)]. (**B**) Photon output (Q) of $Gd_xGa_{1-x}O_z:(SiO_2)_{0.01}$ as a function of x under UV excitation at λ_{max} (256 nm). (**C**) Q of $Gd_3Ga_5O_{12}:(SiO_2)_y$ as a function of y under UV excitation at λ_{max} (256 nm). Spectra were measured with a scanning spectrophotometer consisting of a UV light source (a Xe lamp), a monochromator, a sample scanner, and a spectrograph. To increase data throughput, a liquid N_2-cooled charge-coupled-device camera was used to rapidly measure the spatially dispersed spectrum of each site (in seconds per sample). All scales are in arbitrary units.

Cortical Map Reorganization Enabled by Nucleus Basalis Activity

Michael P. Kilgard* and Michael M. Merzenich

Little is known about the mechanisms that allow the cortex to selectively improve the neural representations of behaviorally important stimuli while ignoring irrelevant stimuli. Diffuse neuromodulatory systems may facilitate cortical plasticity by acting as teachers to mark important stimuli. This study demonstrates that episodic electrical stimulation of the nucleus basalis, paired with an auditory stimulus, results in a massive progressive reorganization of the primary auditory cortex in the adult rat. Receptive field sizes can be narrowed, broadened, or left unaltered depending on specific parameters of the acoustic stimulus paired with nucleus basalis activation. This differential plasticity parallels the receptive field remodeling that results from different types of behavioral training. This result suggests that input characteristics may be able to drive appropriate alterations of receptive fields independently of explicit knowledge of the task. These findings also suggest that the basal forebrain plays an active instructional role in representational plasticity.

The mammalian cerebral cortex is a highly sophisticated self-organizing system (1). The statistics of sensory inputs from the external world are not sufficient to guide cortical self-organization, because the behavioral importance of inputs is not strongly correlated with their frequency of occurrence. The behavioral value of stimuli has been shown to

regulate learning in experiments conducted over more than a century (*2*). Recently, behavioral relevance has been shown to directly modulate representational plasticity in cortical learning models (*3, 4*). The cholinergic nucleus basalis (NB) has been implicated in this modulation of learning and memory. The NB is uniquely positioned to provide the cortex with information about the behavioral importance of particular stimuli, because it receives inputs from limbic and paralimbic structures and sends projections to the entire cortex (*5*). NB neurons are activated as a function of the behavioral significance of stimuli (*6*). Several forms of learning and memory are impaired by cholinergic antagonists and by NB lesions (*7*). Even the highly robust cortical map reorganization that follows peripheral denervation is blocked by NB lesions.

Many studies using acute preparations have shown that electrical stimulation of the NB (*8*) or local administration of acetylcholine (ACh) (*9*) can modulate stimulus-evoked single-unit responses. The variability across studies in the direction, magnitude, and duration of the modulation has made it difficult to relate these effects to long-term cortical map plasticity (*10*).

To clarify the role of the NB in representational plasticity, we investigated the consequences of long-term pairing of tones with episodic NB stimulation. A stimulating electrode was implanted in the right NB of 21 adult rats. After recovery, animals were placed in a sound attenuation chamber and a pure tone was paired with brief trial-by-trial epochs of NB stimulation during daily sessions (*11*). The tone paired with NB stimulation occurred randomly every 8 to 40 s. Pairing was repeated 300 to 500 times per day for 20 to 25 days. The rats were unanesthetized and unrestrained throughout this procedure.

Twenty-four hours after the last session, each animal was anesthetized and a detailed map of the primary auditory cortex (A1) was generated from 70 to 110 microelectrode penetrations (*12*). During this cortical mapping phase, experimenters were blind to the tone frequency that had been paired with NB stimulation. The frequency-intensity response characteristics of sampled neurons were documented in every penetration by presentation of 45 pure tone frequencies at 15 sound intensities. Tuning curves were defined by a blind experienced observer (*13*).

Figure 1A illustrates the organization of A1 in a representative naïve rat. The color

of each polygon denotes each penetration's best frequency (BF), which is the frequency that evoked a neuronal response at the lowest stimulus intensity. The frequency representation is complete and regular in control rats. Each frequency is represented by a band of neurons that extends roughly dorsoventrally across A1. The 9-kHz isofrequency band, for example, is shaded light blue in Fig. 1A, and penetrations with a BF within a third of an octave of 9 kHz are hatched with white. Figure 1B shows the tips of the tuning curves recorded in every

penetration. The tip of the "V" marks the BF; the width of the V denotes the range of frequencies to which the neurons at the site responded at 10 dB above threshold. In naïve rats, BFs were evenly distributed across the entire hearing range of the rat, in accordance with the well-known tonotopic organization of A1 (*14*).

Pairing a specific tonal stimulus with NB stimulation resulted in remodeling of cortical area A1 in all 21 experimental rats. In the representative example shown in Fig. 1C, a 50-dB 9-kHz tone was paired with NB
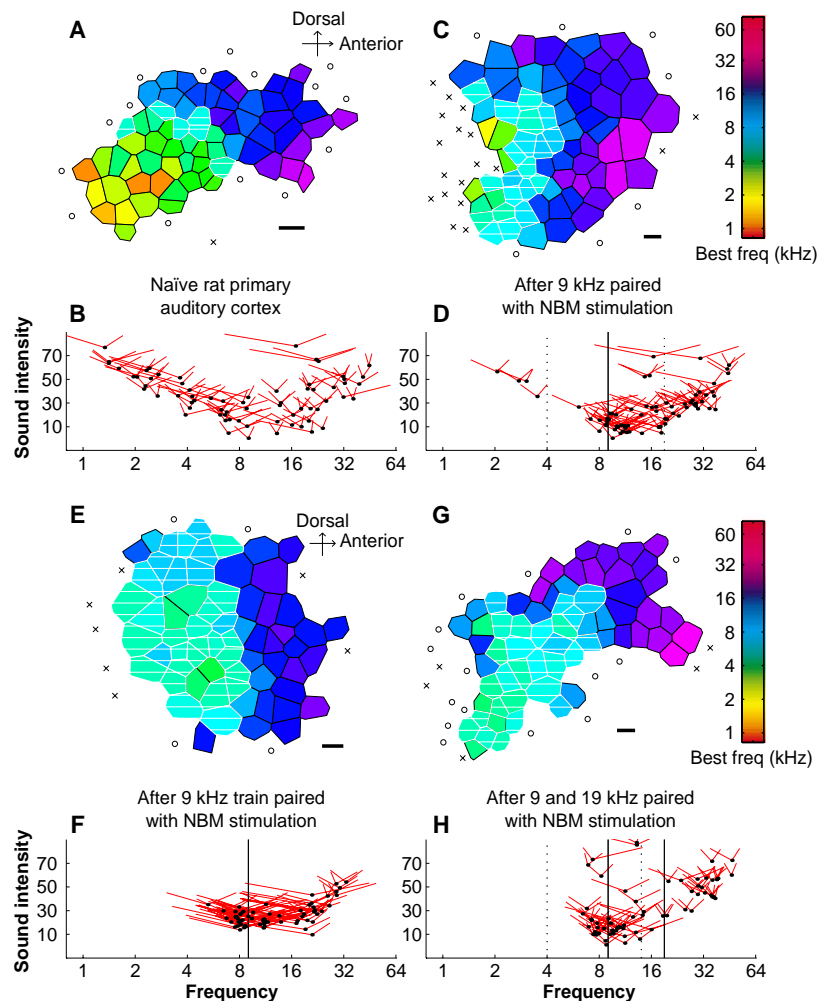
Fig. 1. (**A**, **C**, **E**, and **G**) Representative maps of A1 that show the effects of pairing 9-kHz tones with electrical stimulation of the NB. (A) Representative map from an experimentally naïve rat demonstrating the normal orderly progression of BFs recorded in the rat A1. Each polygon represents one electrode penetration. The color of each polygon indicates the BF in kilohertz. The polygons (Voronoi tessellations) were generated so that every point on the cortical surface was assumed to have the characteristics of the closest sampled penetration. Hatched polygons designate sites with BFs within one-third of an octave of 9 kHz, illustrating a typical isofrequency band. Penetrations that were either not responsive to tones (O) or did not meet the criteria of A1 responses (X) were used to determine the borders of A1. (C) Map of A1 after pairing a 250-ms 9-kHz tone with NB stimulation. (E) Map of A1 after pairing a train of six 9-kHz tones with NB stimulation. (G) Map of A1 after pairing both 9- and 19-kHz tones with NB stimulation. The expansion of the 9-kHz isofrequency band is shown in (C), (E), and (G). Scale bar, 200 μm. (**B**, **D**, **F**, and **H**) Distribution of tuning curve tips at every A1 penetration from each map, which indicate the BF, threshold, and receptive field width 10 dB above the threshold for neurons recorded at each penetration. Threshold as a function of frequency (in kilohertz) matches previously defined behavioral thresholds. Solid vertical lines mark the frequency paired with NB stimulation. Dotted vertical lines mark frequencies presented as often as, but not paired with, stimulation.

Departments of Otolaryngology and Physiology, W. M. Keck Foundation Center for Integrative Neuroscience, University of California, San Francisco, 513 Parnassus Avenue, Box 0732, San Francisco, CA 94143, USA.

*To whom correspondence should be addressed.

stimulation approximately 300 times per day over a period of 20 days. This treatment produced a clear expansion of the region of the cortex that represented frequencies near 9 kHz (Fig. 1C). Figure 1D illustrates the clustering of tuning curve BFs near the frequency that was paired with NB stimulation. After pairing, neurons from 20 of the penetrations into the conditioned map shown in Fig. 1C had BFs within a third of an octave of 9 kHz, compared to only 6 kHz in the equivalently sampled control map. The increase in 9-kHz representation resulted in a clear decrease in the area of A1 that responded to lower frequencies. In the control map, 22 penetrations had BFs less than 5 kHz, compared to only 4 penetra-

tions in the conditioned map. It should be noted that the decrease in low frequency responses is not a consistent finding. In other examples, the low-frequency responses appeared unaltered and the representation of higher frequencies was decreased.

Because the tone paired with NB stimulation was well above the threshold, it was important to examine not only the shifts in the tuning curve tips but also the responses of cortical neurons to tones at the conditioned intensity. During pairing, many of the neurons with BFs different from 9 kHz were excited by the auditory stimulus because most rat A1 tuning curves broaden as intensity is increased. In the naïve map, less than 25% of neurons within A1 responded to 9 kHz presented at 50 dB. By contrast, almost 50% of the conditioned cortex responded to the same stimulus.

Figure 2 summarizes the magnitude of representational changes that resulted from

pairing one frequency with NB stimulation in 10 animals. Figure 2A represents data from seven naïve controls and illustrates the average percent of the surface of A1 that responded to tones at any combination of frequency and intensity. Figure 2, C and D, shows the percent change relative to controls after pairing NB stimulation with 4-, 9-, or 19-kHz tones, respectively. In each case, the cortical area representing the paired stimulus nearly doubled. These results indicate that the responses of tens of thousands or hundreds of thousands of A1 neurons can be altered by pairing tones with NB stimulation in a passively stimulated animal.

In four animals, NB stimulation was paired with a train of six 9-kHz tone pips (25 ms) presented at 15 Hz to test the effects of increasing temporal structure in the auditory stimulus (Fig. 1, E and F). Conditioning with this stimulus unexpect-
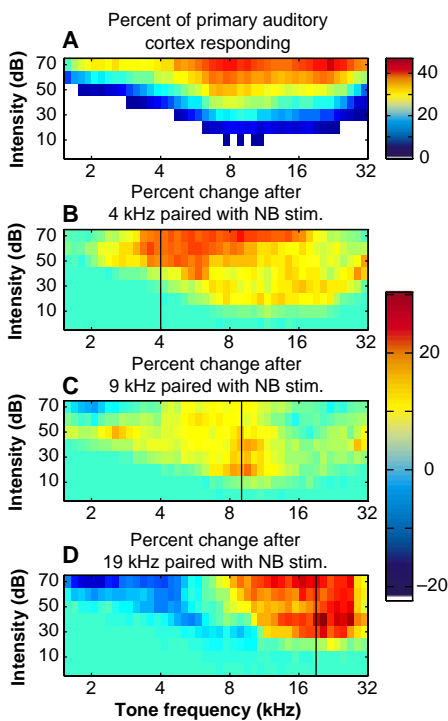
Fig. 2. (**A**) Percent of the surface of A1 that responds to pure tones at each combination of tone frequency and intensity. The average of seven experimentally naïve animals is shown. (**B** through **D**) Percent change in the percent of the primary auditory cortex responding to tones after 1 month of 4-, 9-, or 19-kHz tones paired with NB stimulation ($n = 4$, 4, and 2, respectively). Each group showed a significant increase over controls in the percent responding to the conditioned frequency at 50 dB above the minimum threshold ($P < 0.005$, two-tailed t test). The percent of A1 responding is the sum of the areas of all of the Voronoi tessellations that responded to the particular frequency and intensity combination of interest, divided by the total area of A1. The function is highly reproducible across naïve controls with an average standard error across frequencies of less than 3%. Tessellation was chosen to derive area measurements from discretely sampled points by assuming that each location on the cortical surface had the characteristics of the closest sampled penetration.
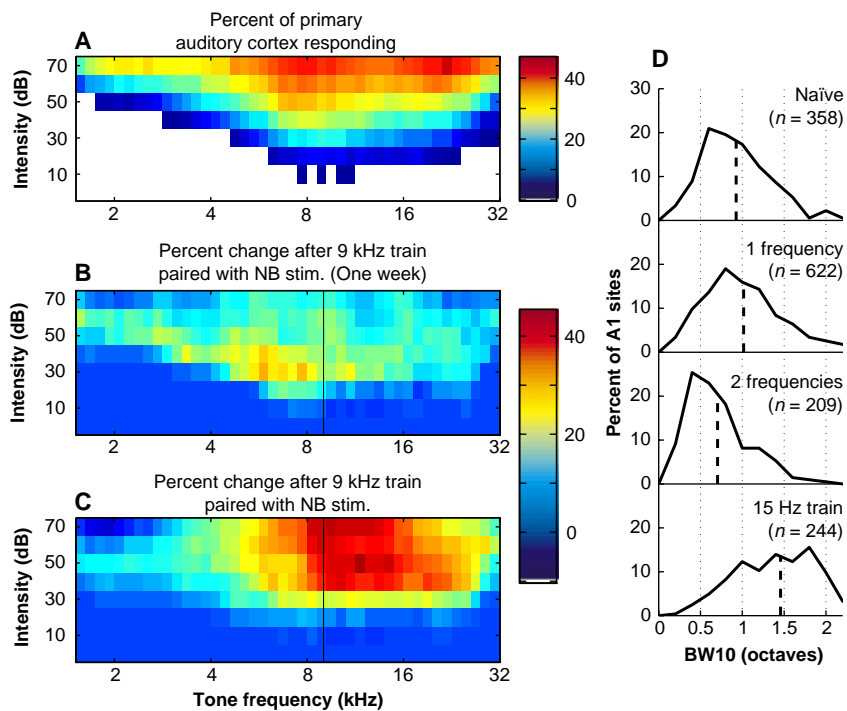
Fig. 3. (**A**) Percent of the surface of A1 that responds to pure tones of any combination of tone frequency and intensity. The average of seven experimentally naïve animals is shown. (**B**) Percent change in the percent of A1 responding after 1 week of pairing 9-kHz tone pip trains (15 Hz) with NB stimulation. There was a significant increase in the response to 9 kHz at 50 dB above the minimum threshold as compared to controls (t test; $n = 2$, $P < 0.05$). (**C**) Percent change in the percent of A1 responding after 1 month of pairing 9-kHz tone pip trains (15 Hz) with NB stimulation. There was a significant increase in the response to 9 kHz at 50 dB above the minimum threshold as compared to controls ($n = 4$, $P < 0.00001$). (**D**) Distribution of receptive field width BW10 for every A1 penetration for each of the four classes of experiments. Pairing one frequency with NB stimulation did not significantly effect the BW10 distribution relative to naïve animals, whereas pairing two frequencies (4 and 14, or 9 and 19 kHz) or a 15-Hz train of stimuli caused receptive field width to be decreased and increased, respectively. The same effect is present in the distributions of BW20 to BW40. The dashed vertical line marks the mean of each distribution. Single units were sorted from the multi-unit data derived from the four naïve animals (15 units) and from four train-conditioned animals (33 units). The mean BW10 for single units was also increased by 15-Hz train conditioning (0.91 versus 1.38 octaves, $P < 0.005$). This widening of tuning curves adds with the BF shifts to generate the large increase in the percent of A1 responding after train conditioning.

edly resulted in even greater cortical reorganization than conditioning with a 250-ms tone ($P < 0.01$, Fig. 3C). In the example shown, the 9-kHz isofrequency band was increased from roughly 250 μm wide in a naïve A1 to more than 1 mm wide. After pairing, over 85% of A1 responded to 9 kHz at 50 dB. Additionally, 50% of A1 penetrations had best frequencies within one-third of an octave of 9 kHz, compared to less than 15% in the control animals. The extent of cortical map reorganization generated by NB activation is substantially larger than the reorganization that is typically observed after several months of operant training (15–17).

The six short tones presented at 15 Hz evoked less than 30% more spikes than did a single tone, because most rat A1 neurons do not follow onsets presented faster than 12 to 14 Hz (18). It seems unlikely that the larger reorganization evoked with stimulus trains is simply due to an increased cortical response to the stimuli.

Two animals were mapped after only 1 week of conditioning with the 15-Hz stimulus to examine the rate of cortical remodeling evoked by NB activation. The 9-kHz representation was increased by 18% after 1 week of training. This reorganization was nearly halfway to the 44% increase that was recorded after a month of conditioning, indicating that the cortical remodeling generated by NB stimulation was progressive in nature (Fig. 3B).

To probe the competitive processes underlying cortical reorganization, five rats were conditioned with two different randomly interleaved tones that were more than an octave apart. Two distinct classes of reorganizations resulted. The tuning curve tips were either shifted toward a point between the two conditioned frequencies, so that both were within the receptive field at 50 dB ($n = 3$), or shifted toward only one of the two conditioned frequencies ($n = 2$, Fig. 1, G and H). The two classes of results may be the consequence of subtle variations in A1 before NB pairing, which can have large effects when competitive processes are involved.

To document the fact that NB activation is required for the cortical reorganizations observed in this study, during four of our experiments two additional frequencies were delivered on identical presentation schedules as the paired tones but were not paired with NB stimulation. These stimuli, which never occurred within 8 s of NB stimulation, did not measurably affect cortical responses or representations (19).

Microdialysis experiments have shown that electrical stimulation of the NB results in ACh release in the cortex (20). Additionally, both the short-term plasticity and the electroencephalogram (EEG) desynchronization evoked by NB stimulation are blocked by atropine (21). Thus, the cortical plasticity demonstrated in this study likely involves the release of cortical ACh paired with tones. To test for the necessity of ACh release in our model, a 19-kHz tone was paired with electrical stimulation of the NB in animals with highly specific lesions of the cholinergic NB neurons (22). No significant increase in the 19-kHz representation was observed in lesioned animals. Even though ACh release is clearly important for NB function, it may be too simplistic to focus exclusively on ACh because only one-third of NB projection neurons are cholinergic (23). One-third use γ-amino butyric acid and the remaining third are uncharacterized. Future work is needed to elucidate the function of concurrent release of these transmitters in cortical plasticity.

The nature of the auditory stimuli paired with NB activation had a profound effect on the selectivity of cortical responses (Fig. 3D). Sharpness of tuning was quantified as the width of the tuning curve 10 dB above the threshold (BW10). When a 250-ms tone was used as the conditioning stimulus, the average BW10 was not significantly different from the average BW10 of control rats (0.93 versus 1.02 octaves). Conditioning with a temporally modulated stimulus (a train of six short tones of the same frequency) resulted in a mean cortical response that was less selective than in controls (1.46 octaves, $P < 0.0001$). Conditioning with two tones engaging different spatial locations on the input array (the cochlea) resulted in cortical responses that were more selective than in controls (0.70 octaves, $P < 0.0001$). Thus, our model results in receptive fields that are narrowed, broadened, or unaltered depending on specific parameters of the acoustic stimulus paired with NB stimulation.

Similar increases and decreases in receptive field sizes have been recorded in the somatosensory and auditory cortices of New World monkeys that have been trained at tactile or auditory discrimination, detection, or time-order judgment tasks (4). A pure tone discrimination task or a task involving a stimulus that moved across several fingers decreased receptive field diameters by approximately 40% (15, 16). In contrast, a task that required detection of differences in the amplitude modulation rate of tactile stimuli delivered to a constant skin surface increased receptive field diameters by more than 50% (17).

The mechanisms responsible for remodeling receptive fields in a manner that is appropriate for the particular task that an animal practices are not well defined. One possibility is that top-down instruction from a higher cortical field with explicit knowledge of the goals of the operant task directs cortical plasticity. The fact that our simple model, without any behavioral task, can generate the same receptive field effects as are induced by extended periods of operant training suggests that the characteristics of the stimuli paired with subcortical neuromodulatory input are sufficient to determine the direction of receptive field alterations (24).

Adult cortical plasticity appears to be responsible for improvements in a variety of behavioral skills, maintenance of precise sensory representations, compensation for damage to sensory systems, and functional recovery from central nervous system damage (4). Our results suggest that activation of the NB is sufficient to guide both large-scale cortical reorganization and receptive field reorganization to generate representations that are stable and adapted to an individual's environment by labeling which stimuli are behaviorally important.

REFERENCES AND NOTES

1. W. Singer. *Eur. Arch. Psych. Neurol. Sci.* **236**, 4 (1986).
2. E. L. Thorndike, *Animal Intelligence* (Macmillan, New York, 1911).
3. E. Ahissar *et al.*, *Science* **257**, 1412 (1992); N. M. Weinberger, *Curr. Opin. Neurobiol.* **3**, 570 (1993); E. Ahissar and M. Ahissar, *ibid.* **4**, 80 (1994).
4. M. M. Merzenich, G. H. Recanzone, W. M. Jenkins, K. A. Grajski, *Cold Spring Harbor Symp. Quant. Biol.* **55**, 873 (1990).
5. M. M. Mesulam, E. J. Mufson, B. H. Wainer, A. I. Levey, *Neuroscience* **10**, 1185 (1983); D. B. Rye, B. H. Wainer, M. M. Mesulam, E. J. Mufson, C. B. Saper, *ibid.* **13**, 627 (1984); M. Steriade and D. Biesold, *Brain Cholinergic Systems* (Oxford Univ. Press, New York, 1990).
6. R. T. Richardson and M. R. DeLong, in *Activation to Acquisition. Functional Aspects of the Basal Forebrain Cholinergic System* (Birkhauser, Boston, 1991), pp. 135–166; R. T. Richardson and M. R. DeLong, *Adv. Exp. Med. Biol.* **295**, 233 (1991); A. E. Butt, G. Testylier, R. W. Dykes, *Psychobiology* **25**, 18 (1997).
7. R. C. Peterson, *Psychopharmacology* **52**, 283 (1977); H. H. Webster, U. Hanisch, R. W. Dykes, D. Biesold, *Somatosens. Mot. Res.* **8**, 327 (1991); A. E. Butt and G. K. Hodge, *Behav. Neurosci.* **9**, 699 (1995); G. Leanza *et al.*, *Eur. J. Neurosci.* **8**, 1535 (1996); K. A. Baskerville, J. B. Schweitzer, P. Herron, *Neuroscience* **80**, 1159 (1997).
8. R. Metherate and J. H. Ashe, *Brain Res.* **559**, 163 (1991); *Synapse* **14**, 132 (1993); J. M. Edeline, C. Maho, B. Hars, E. Hennevin, *Brain Res.* **636**, 333 (1994); J. M. Edeline, B. Hars, C. Maho, E. Hennevin, *Exp. Brain Res.* **97**, 373 (1994).
9. R. Metherate, N. Tremblay, R. W. Dykes, *J. Neurophysiol.* **59**, 1231 (1988); T. M. McKenna, J. H. Ashe, N. M. Weinberger, *Synapse* **4**, 30 (1989); R. Metherate and N. M. Weinberger, *Brain Res.* **480**, 372 (1989); *Synapse* **6**, 133 (1990).
10. Although studies using stimulation of the NB reported mostly facilitation of the response to the paired stimulus, in several studies using local administration of ACh to alter receptive field organization the opposite effect was reported. In these studies, ACh most often caused a significant stimulus-specific decrease in cortical responsiveness after the pairing procedure. The average duration of the plasticity also varied across studies from less than 10 min to more than 1 hour.

11. Platinum bipolar stimulating electrodes were lowered 7 mm below the cortical surface 3.3 mm lateral and 2.3 mm posterior to the bregma in barbiturate-anesthetized rats weighing ~300 g and were cemented into place with the use of sterile techniques approved under animal care protocol of the University of California, San Francisco. After 2 weeks of recovery, 250-ms (or a 15-Hz train of six 25-ms) 50-dB sound pressure level tones were paired with 200 ms of NB electrical stimulation in a sound-shielded, calibrated test chamber (5 days per week). Electrical stimulation began either 50 ms after tone onset ($n = 15$) or 200 ms before ($n = 6$). The two timings did not appear to affect plasticity, and data from both groups were pooled. The current level (70 to 150 μA) was chosen to be the minimum necessary to desynchronize the EEG during slow-wave sleep for 1 to 2 s. Stimulation consisted of 100-Hz capacitively coupled biphasic pulses of 0.1 ms duration. Tonal and electrical stimuli did not evoke any observable behavioral responses (that is, did not cause rats to stop grooming or if sleeping, awaken).

12. Twenty-four hours after the last pairing, animals were anesthetized with pentobarbital and the right auditory cortex was surgically exposed. Parylene-coated tungsten microelectrodes (2 megohms) were lowered 550 μm below the pial surface (layer 4/5), and complete tuning curves were generated with 50-ms pure tones (with 3-ms ramps) presented at 2 Hz to the contralateral ear. The evoked spikes of a small cluster of neurons were collected at each site. To determine the effects of conditioning on the bandwidth of individual neurons, spike waveforms were collected during eight experiments and were sorted offline with software from Brainwave Technologies. Penetration locations were referenced using the cortical vasculature as landmarks. The primary auditory cortex was defined on the basis of its short latency (8- to 20-ms) responses and continuous tonotopy (BF increases from posterior to anterior). Responsive sites that exhibited clearly discontinuous BFs and either long latency responses, an unusually high threshold, or very broad tuning were considered to be non-A1 sites. Penetration sites were chosen to avoid blood vessels while generating a detailed and evenly spaced map. The edges of the map were estimated with the use of a line connecting the nonresponsive and non-A1 sites. Map reorganizations resulted in significant effects on the outline of A1, although no particular pattern was observed. The effect of conditioning on mean bandwidths across all conditions was determined with analysis of variance; pairwise comparisons were analyzed by Bonferroni post-hoc tests.

13. The set of tone frequencies presented at each site was approximately centered on the BF of each site. Thus, during analysis each tuning curve was approximately centered in the stimulus space, and simply blanking the axes and analyzing the sites in random order allowed for tuning curve characterization to be completely blind. With the use of custom analysis software, the tuning curve edges for each site were defined by hand and recorded without the possibility of experimenter bias.

14. S. L. Sally and J. B. Kelly, *J. Neurophysiol.* **59**, 1627 (1988).

15. G. H. Recanzone, C. E. Schreiner, M. M. Merzenich, *J. Neurosci.* **13**, 87 (1993).

16. W. M. Jenkins, M. M. Merzenich, M. T. Ochs, T. Allard, E. Guic-Robles, *J. Neurophysiol.* **63**, 82 (1990).

17. G. H. Recanzone, M. M. Merzenich, W. M. Jenkins, K. A. Grajski, H. R. Dinse, *ibid.* **67**, 1031 (1992).

18. M. P. Kilgard and M. M. Merzenich, unpublished observation.

19. In contrast to the large changes induced by pairing tones with NB stimulation, no significant cortical map reorganizations were observed in previous experiments after tens of thousands of behaviorally irrelevant stimuli were presented over 3 to 5 months (*14, 16*). Additionally, short-term repetition of one frequency without behavioral relevance (habituation) results in a dramatic decrease in A1 responses to that frequency [C. D. Condon and N. M. Weinberger, *Behav. Neurosci.* **105**, 416 (1991)]. These studies suggest that stimulus presentation without behavior-al importance does not result in significant map changes. Although it is unlikely to be a contributing factor, we acknowledge that we did not record from animals that experienced extensive stimulus presentation without any NB stimulation.

20. F. Casamenti, G. Deffenu, A. L. Abbamondi, G. Pepeu, *Brain Res. Bull.* **16**, 689 (1986); D. D. Rasmusson, K. Clow, J. C. Szerb, *Brain Res.* **594**, 150 (1992); M. E. Jimenez-Capdeville, R. W. Dykes, A. A. Myasnikov, *J. Comp. Neurol.* **381**, 53 (1997).

21. B. Hars, C. Maho, J. M. Edeline, E. Hennevin, *Neuroscience* **56**, 61 (1993); J. S. Bakin and N. M. Weinberger, *Proc. Natl. Acad. Sci. U.S.A.* **93**, 11219 (1996).

22. The cholinergic neurons of the NB were selectively destroyed by infusion of 2.5 μg of 192 immunoglobulin G–saporin immunotoxin into the right lateral ventricle before the surgery to implant the stimulating electrode. The toxin, an antibody to the low-affinity nerve growth factor receptor linked to a ribosome-inactivating toxin, has been shown to specifically destroy most of the cholinergic neurons of the basal forebrain projecting to the cortex, while sparing the parvalbumin-containing neurons as well as cholinergic neurons that project from the NB to the amygdala [S. Heckers *et al.*, *J. Neurosci.* **14**, 1271 (1994)]. Electrical stimulation of the NB and tone presentation were identical for lesioned and nonlesioned animals. The percent of the cortex responding to a 19-kHz tone after pairing in lesioned animals was not significantly different from that in naïve controls (two-tailed *t* test, $n = 2$).

23. I. Gritti, L. Mainville, M. Mancia, B. E. Jones, *J. Comp. Neurol.* **383**, 163 (1997).

24. Complex considerations of the network, cellular, and molecular mechanisms responsible for the plasticity observed in our studies are beyond the scope of this report. See M. E. Hasselmo and J. M. Bower, *Trends Neurosci.* **16**, 218 (1993); M. Sarter and J. P. Bruno, *Brain Res. Rev.* **23**, 28 (1997); R. W. Dykes, *Can. J. Physiol. Pharmacol.* **75**, 535 (1997).

25. Supported by NIH grant NS-10414, Hearing Research Inc., and an NSF predoctoral fellowship. We thank C. Schreiner for technical advice and D. Buonomano, H. Mahncke, D. Blake, C. deCharms, C. Schreiner, and K. Miller for helpful comments on the manuscript.

28 October 1997; accepted 23 January 1998

Activation of the OxyR Transcription Factor by Reversible Disulfide Bond Formation

Ming Zheng, Fredrik Åslund, Gisela Storz*

The OxyR transcription factor is sensitive to oxidation and activates the expression of antioxidant genes in response to hydrogen peroxide in *Escherichia coli*. Genetic and biochemical studies revealed that OxyR is activated through the formation of a disulfide bond and is deactivated by enzymatic reduction with glutaredoxin 1 (Grx1). The gene encoding Grx1 is regulated by OxyR, thus providing a mechanism for autoregulation. The redox potential of OxyR was determined to be –185 millivolts, ensuring that OxyR is reduced in the absence of stress. These results represent an example of redox signaling through disulfide bond formation and reduction.

Reactive oxygen species can damage DNA, lipid membranes, and proteins and have been implicated in numerous degenerative diseases (*1*). As a defense, prokaryotic and eukaryotic cells have inducible responses that protect against oxidative damage (*2*). These antioxidant defense systems have been best characterized in *Escherichia coli*, in which the OxyR and SoxR transcription factors activate antioxidant genes in response to H_2O_2 and to superoxide-generating compounds, respectively.

The mechanisms of redox-sensing and the systems that control the redox status of the cell are likely to be coupled. Studies of the thiol-disulfide equilibrium of the cytosol of both prokaryotic and eukaryotic cells indicate that the intracellular environment is reducing, such that protein disulfide bonds rarely occur (*3–5*). The redox potential of the *E. coli* cytosol has been estimated to be approximately –0.26 to –0.28 V (*4, 5*). This reducing environment is maintained by the thioredoxin and the glutaredoxin systems (*6, 7*).

In response to elevated H_2O_2 concentrations, the OxyR transcription factor rapidly induces the expression of *oxyS* (a small, nontranslated regulatory RNA), *katG* (hydrogen peroxidase I), *gorA* (glutathione reductase), and other activities likely to protect the cell against oxidative stress (*2, 8*). Purified OxyR is directly sensitive to oxidation. Only the oxidized form of OxyR can activate transcription in vitro, and footprinting experiments indicate that oxidized and reduced OxyR have different conformations (*9, 10*). Thus, we examined the chemistry of OxyR oxidation and reduction.

No transition metals were detected by inductively-coupled plasma metal ion analysis of two preparations of OxyR (*11*). We also did not observe any change in OxyR activity after denaturation and renaturation in the presence of the metal chelator des-

M. Zheng and G. Storz, Cell Biology and Metabolism Branch, National Institute of Child Health and Human Development, National Institutes of Health, Bethesda, MD 20892, USA.
F. Åslund, Department of Microbiology and Molecular Genetics, Harvard Medical School, Boston, MA 02115, USA.

*To whom correspondence should be addressed. E-mail: storz@helix.nih.gov